

New frequency-modulation readout based on relaxation oscillations

Miha Furlan^{*}, Eugenie Kirk, and Alex Zehnder

Paul Scherrer Institute, Laboratory for Astrophysics, 5232 Villigen PSI, Switzerland

Abstract

Scaling of multi-pixel cryogenic detectors for imaging becomes increasingly difficult with size due to complexity of readout circuitry and cryogenic constraints (thermal load from wiring). We propose and demonstrate a new readout scheme based on a highly stable RF oscillator composed of a superconducting tunnel junction which exhibits relaxation oscillations. The oscillation frequency is almost linear with the analog bias signal over a wide operation range. The frequency signals from different detectors can be combined into one single readout line. The current noise of an optimized circuit is about $5 \text{ pA}/\sqrt{\text{Hz}}$, which is comparable to standard SQUID amplifiers. We show experimental data from ‘stand-alone’ operation as well as response to microcalorimeter X-ray signals.

Key words: relaxation oscillations, analog-to-frequency converter, superconducting tunnel junction, detector readout
PACS: 85.25.Oj, 85.25.Hv, 84.30.Qi, 74.40.+k

Cryogenic radiation detectors have proven to be the devices of choice when highest energy sensitivity (in the X-ray range), single photon detection efficiency and direct spectroscopic resolution are required. For astrophysical observations, a trend toward large arrays for imaging has been accompanied by efforts to solve the non-trivial problem of cryogenic multiple-channel readout. While most readout schemes are based on multiplexed SQUID amplifiers, we propose and demonstrate an alternative and relatively simple low-noise analog-to-frequency conversion circuit.

The operating principle is based on a hysteretic superconducting tunnel junction (STJ) exhibiting relaxation oscillations [1] in the RF range. If the gaps Δ_1 and Δ_2 of the two superconducting elec-

trodes differ slightly ($0 < |\Delta_1 - \Delta_2| \ll \Delta_1, \Delta_2$), the current-voltage characteristics of the device show a region with negative differential resistance where biasing of the device is potentially unstable [2]. An oscillator circuit can be built with an STJ (normal resistance R_n , capacitance C_j and critical current I_c) in series with an inductor L , and voltage biasing both at V_s by a shunt $R_s \ll R_n$, as depicted in the inset of Fig. 1.

Operating the circuit at a current $I_b > I_c$ determined by the current limiting resistor $R_b \gg R_s$ the relaxation oscillations are dominated by [1,3] – the current rise time

$$\tau_{sc} = -\frac{L}{R_s} \ln(1 - \alpha^{-1}) \quad (1)$$

on the supercurrent (SC, zero voltage) branch of the current-voltage curve, where $\alpha = I_b/I_c$ is the normalized bias parameter, and

^{*} Corresponding author. Tel.: +41-56-310-4519.
Email address: miha.furlan@psi.ch (Miha Furlan).

– the current decay time

$$\tau_{qp} = \frac{L}{R_s + R_{qp}} \ln \left(1 + \frac{(R_s + R_{qp})I_c}{V_g - V_s} \right) \quad (2)$$

on the quasiparticle (QP) branch at the gap voltage $V_g = (\Delta_1 + \Delta_2)/e$, where R_{qp} is the junction resistance in the gap region.

The voltage switching times between SC and QP branch are on the order of $\tau_v \approx C_j V_g / I_c$ and are usually negligibly fast. For $V_s \ll V_g$ and $R_{qp} \gg R_s$ we find $\tau_{sc} \gg \tau_{qp}$ which yields an approximation for the relaxation oscillation frequency:

$$\begin{aligned} f_r &= \frac{R_s}{L} \left(\alpha - \frac{1}{2} - O(\alpha^{-1}) \right) \\ &= \frac{V_s}{I_c L}, \quad (\alpha \gg 1). \end{aligned} \quad (3)$$

Hence, f_r is proportional to V_s (or to $I_b = V_s / R_s$) and the circuit behaves as an almost linear analog-to-frequency converter over an acceptably broad dynamic range.

Relaxation oscillations have been measured at 100 mK for various circuit parameters. Experimental $f_r(V_s)$ dependence for different critical currents $I_c = I_c^0 / \kappa$ is shown in Fig. 1, where the nominal value I_c^0 may be suppressed by a factor κ to the effective I_c due to application of a magnetic field. This is particularly convenient for tuning of the

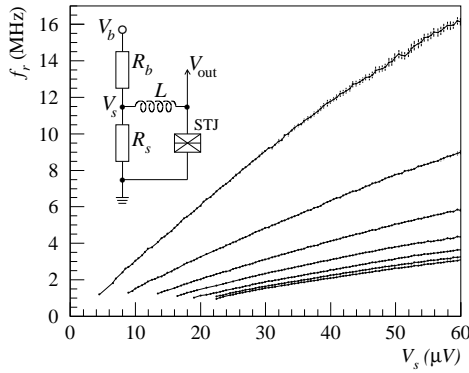


Fig. 1. Measured f_r as a function of V_s and for different I_c (modified by application of magnetic field). Fitting the theoretical f_r to the data points yielded (from bottom to top): $I_c = 58.07, 53.71, 48.15, 39.55, 29.98, 19.69,$ and $10.63 \mu\text{A}$ ($I_c^0 = 58.3 \mu\text{A}$). The circuit parameters were: $L = 280 \text{ nH}$, $R_s = 91 \text{ m}\Omega$, and the STJ having $V_g = 330 \mu\text{V}$ and $R_n = 1.2 \Omega$.

circuit behaviour or eventually extending the operation range to lower currents. The deviation from linearity observed in Fig. 1 is fully accounted for by using both Eqs. (1) and (2), because τ_{qp} starts to contribute at higher V_s .

If we now introduce a cryogenic detector by replacing R_b with a high-resistance device (e.g. a NIS microcalorimeter) or R_s with a low-resistance device (e.g. a TES), the detector signal will be directly converted to a change in f_r . The oscillator signal V_{out} with relatively large amplitude V_g is demodulated with conventional (phase-locked loop) electronics outside the cryostat. The measured response of the oscillator to a SINIS detector [4] X-ray event is shown in Fig. 2.

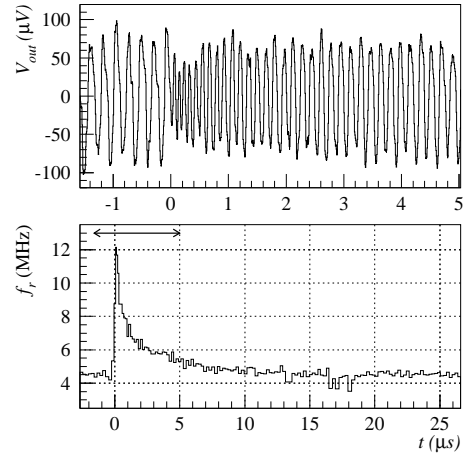


Fig. 2. Top: Relaxation oscillations during a SINIS detector 6 keV X-ray event (the detector replacing R_b). The amplitude modulation and sinusoidal oscillation are due to the externally applied band-pass filter. Bottom: Time sequence of inverse oscillation periods, equivalent to a time-dependent f_r , extracted from the above analog signal (note the larger time scale, while the arrow indicates the range of the top graph). Circuit and device parameters were: $L = 48 \text{ nH}$, $R_s = 91 \text{ m}\Omega$, $I_c = 7.28 \mu\text{A}$ ($\kappa = 8$).

The detector was biased close to its gap voltage ($V_d = 2\Delta_{\text{Al}}/e$) at $V_b = 334 \mu\text{V} = 0.98 V_d$ for operation at sufficiently high dark current $I_b^0 = 17.5 \mu\text{A} = 2.4 I_c$. The peak current of the measured analog signal was $I_b^1 = 46.4 \mu\text{A}$ (the indices 0 and 1 denote the dark and irradiated detector states, respectively). The corresponding frequencies extracted from Fig. 2 are $f_r^0 = 4.47 \text{ MHz}$ and $f_r^1 = 12.1 \text{ MHz}$, which, using Eq. (3), give currents

of $17.2 \mu\text{A}$ and $46.5 \mu\text{A}$, respectively. There is excellent agreement between analog and frequency-modulated signals, which is particularly remarkable considering the model simplifications and experimental uncertainties. The relative width $\langle \delta\tau_r \rangle / \langle \tau_r \rangle$ of the oscillation period distribution (in ‘stand-alone’ operation without noisy detector) was typically on the order of 10^{-2} .

For observation of stable relaxation oscillations and optimum noise behaviour, several constraints on circuit parameters have to be considered [3], a discussion of which is beyond the scope of this paper. Nevertheless, we present calculations and realistic estimates for the proposed circuit including standard (SI)NIS and TES detectors.

The main noise sources from the oscillator are Johnson noise from R_s , shot noise from tunneling, $1/f$ flicker noise from two-level fluctuators [5] and thermally activated escape from the zero-voltage state [6]. For typical STJ devices and high-frequency operation the process of thermal excitation over an energy barrier was found to dominate the circuit noise. Depending on junction parameters, temperature T , and current slew rate $dI/dt \approx I_c/\tau_{sc}$ the transitions from the superconducting to the resistive states will occur at a current $I_m < I_c$. The width $\langle \delta I_m \rangle / I_c$ of the transition current probability function is, to first order, proportional to $(T/I_c)^{2/3}$ [7]. Critical-current fluctuations are a direct linear cause for fluctuations of the relaxation oscillation period $\delta\tau_r/\tau_r = \delta I_m/I_m$, and we can determine a current noise density (referred to the circuit input and valid over a limited parameter range [3]) of

$$j_b = \frac{I_b}{\sqrt{f_r}} \frac{\delta\tau_r}{\tau_r} = \frac{\alpha I_c}{\sqrt{f_r}} \frac{\delta I_m}{I_m} \propto \frac{\alpha I_c^{1/3} T^{2/3}}{f_r^{1/2}}. \quad (4)$$

Table 1 summarizes calculated optimum parameters for realistic (SI)NIS and TES readout. For the current-to-voltage converter (NIS readout) we have chosen the smallest STJ dimensions which can still be easily fabricated by standard optical lithography. In the case of TES readout we are restricted to a typical resistance R_s of the detector. The current-noise levels j_b in Table 1 are sufficiently low compared to detector or SQUID noise.

The most apparent advantages of the relaxation

Table 1

Examples of optimum STJ and circuit parameters for readout of NIS and TES detectors, where ℓ is the STJ side length (see main text for the other parameters). In the TES case R_s corresponds to the detector itself with a typical operating point resistance. Both circuits are operated at $T = 100 \text{ mK}$ and $\alpha = 3$.

	ℓ	R_n	κ	I_c	L	R_s	f_r	$\frac{\delta\tau_r}{\tau_r}$	j_b
	(μm)	(Ω)		(μA)	(μH)	(Ω)	(MHz)	($\cdot 10^3$)	$\left(\frac{\text{pA}}{\sqrt{\text{Hz}}}\right)$
NIS	5	40	12	0.52	0.8	8	30	17	5.1
TES	20	2.5	15	6.68	0.1	0.1	3	3.1	37

oscillation based readout compared to existing technologies are that it neither requires narrow band filtering as in frequency-domain multiplexing, nor does it suffer from switching complications as in time-domain multiplexing. Furthermore, there is no need for complex bias and control circuitry. The main disadvantage of our TES readout scheme is the operation in the less favoured and potentially unstable current biasing mode. Finally, this scheme is probably not appropriate for readout of STJ detectors due to their intrinsically low current levels compared to I_c of the oscillator STJ.

Acknowledgements We are indebted to Ph. Lerch for valuable discussions and to F. Burri for technical support.

References

- [1] F.L. Vernon and R.J. Pedersen, J. Appl. Phys. **39** (1968) 2661.
- [2] I.Kh. Albegova et al., Zh. Tekh. Fiz. **39** (1969) 911 [Sov. Phys. Tech. Phys. **14** (1969) 681].
- [3] A detailed model description, calculations of circuit dynamics and a broad discussion on noise are presented elsewhere [M. Furlan et al., paper in preparation].
- [4] M. Furlan, E. Kirk, and A. Zehnder, these proceedings.
- [5] F.C. Wellstood, C. Urbina, and J. Clarke, Appl. Phys. Lett. **85** (2004) 5296.

- [6] T.A. Fulton and L.N. Dunkleberger, Phys. Rev. B **9** (1974) 4760.
- [7] O.V. Snigirev, IEEE Trans. Magn. **19** (1983) 584.